

# Design of a Laboratory Scale Archimedes Screw Turbine Model Hydroelectric Power Station (PLTA) Simulator

Muhammad Hasan Basri, Ahmad Muhtadi, Darul Hasan

Department of Electrical Engineering, Universitas Nurul Jadid, Paiton, Probolinggoand 67291, Indonesia

## ARTICLE INFO

### Article history:

Received May 30, 2023

Revised July 08, 2023

Published July 12, 2023

### Keywords:

Renewable energy;  
Archimedes Screw Turbine;  
Efficiency evaluation;  
Cheap installation.

## ABSTRACT

The purpose of this research is to design a new model simulator of the Archimedes Screw turbine on a laboratory scale which is simple, inexpensive, environmentally friendly and for practice at the Electrical Engineering Laboratory of Nurul Jadid University by studying the efficiency of the Archimedes turbine which utilizes kinetic energy. water flow energy from the difference in upstream-downstream water head. Methods used numerical simulations have been run to evaluate the performance coefficient of the turbine alone (without friction loss or blockage augmentation), and to extend the TSR range. Numerical simulations make it possible to generate efficiency curves of Archimedes Screw turbines in both parallel and inclined configurations. The result obtained is that the proposed geometry can be used in real-life applications, providing 0.5 kW at flow velocities between 1 and 2 m/s. Novelty of hydropower simulation studies of the Archimedes turbine screw model using numerical simulation methods.

This work is licensed under a [Creative Commons Attribution-Share Alike 4.0](https://creativecommons.org/licenses/by-sa/4.0/)



## Corresponding Author:

Muhammad Hasan Basri, Department of Electrical Engineering, Universitas Nurul Jadid, Paiton, Probolinggoand 67291, Indonesia  
Email: [hasanmohammadbasri83@gmail.com](mailto:hasanmohammadbasri83@gmail.com).

## 1. INTRODUCTION

One of the fundamental societal challenges for the coming decades is the use of renewable energy resources, towards sustainable development [1]. Screw Turbine or Archimedean Screw is a turbine that existed in ancient times which was used as a water pump for irrigation. Along with the energy crisis and the limited energy potential of high-head water, in 2007 an engineer modified the Archimedes pump which was reversed and let the water control the pump and a generator was installed at the end of the pump, so it can produce electricity as long as the generator is not submerged in water or exposed to water [2].

Vermaak *et al.* [3] looked at the technical, economic and environmental uses of micro-hydro river technology, which can work with little or no water. To evaluate the best option for rural power supply, a simulation program is used in reference [4], [5], compared micro-hydro power with wind, photovoltaic and diesel generators. Micro-hydro power was found to be the best option, where water resources are available, cost-effective and reduces CO<sub>2</sub> input to the atmosphere. Therefore, this renewable technology provides a cost-effective source of electricity in rural areas, where distances are long, the population is small and the demand for energy is low. Moreover, the small Archimedean Screw power system reduces the number and size of infrastructure normally required by hydroelectric power plants (as described in Ref. [6]. This absence of permanent infrastructure, 1) reduces the impact on the ecosystem and, 2) facilitates installation and maintenance in the area. isolated.

The advantages possessed by the Archimedes Screw turbine compared to other types of turbines are as follows: a) Well developed in areas that have water sources with a large enough discharge (rivers) but only have a low head, b) Does not require a very high control system complicated like other turbines, c) The water pressure that occurs in the turbine does not damage the ecology in this case the impact on aquatic living things (fish), d) It does not require a design, so it can reduce expenses for digging installation of the design, e) Has high efficiency, with large discharge variations and very good for small water debits, f) Does not require fine

mesh to prevent debris from entering the turbine, thereby reducing maintenance costs [7]. Various reviews of hydrokinetic power systems are available. For example, Khan *et al.* [8], [9] provide an overview of the vertical axis and horizontal axis hydrokinetic turbines. Kumar and Sarkan [10] reviewed a large number of hydrokinetic energy conversion systems. Rostami and Fernandez proposed a vertical flat plate, free to rotate about the vertical axis of symmetry, to exploit autorotation caused by vortex shedding [11]. Finally, a review of vertical axis autorotating current turbines is reported in Ref. [12].

In this discussion, the Archimedes Screw turbine can have an important role. These have long been used in micro-hydro power plants, with very high efficiencies (up to 85%, as reported in ref [13], where traditional systems are described), but were classified as reaction turbines as distinct from hydrokinetic turbines in Okot's review [14]. gradient between the two ponds and never used in free flow. In view of its high performance, it is also applied in duct systems. For example, Rigling, Schleicher, and coworkers evaluated numerically the efficiency of the unequal Archimedean spiral rotor in Ref. [15], found the best hydraulic efficiency point of 72%. In both traditional and canal conditions, the system requires a set of structures, this has a significant environmental impact and makes the use of the technology in remote areas inconvenient. The generator used is a generator with a permanent magnet where the excitation source is based on a permanent magnet on the rotor [23]. Literature on Archimedes Screw turbines is abundant. The first attempt using an Archimedes Screw turbine was proposed by Stergiopoulou and co-workers [16], [17], but their work did not provide an accurate evaluation of the efficiency of the Archimedes Screw turbine or comparison with other Archimedes Screw turbines. The output power generated from the screw turbine depends on the geometry of the turbine. There are two parameters that affect the geometry, namely external parameters such as the length of the turbine, outside radius and slope, and internal parameters such as the radius of the blades, the number and spacing of the blades [18].

The use of the axial Archimedes Screw turbine completely changes its operating principle: the traditional Archimedes screw turbine discharges the difference in potential energy between two water tanks, while the Archimedes Screw turbine exploits the kinetic energy of the flow. Apart from the geometric differences between the various Archimedes Screw turbines, the evaluation of the efficiency of the Archimedes Screw turbines is based on the Betz one-dimensional model [19], [20], Can be seen in Fig. 1.

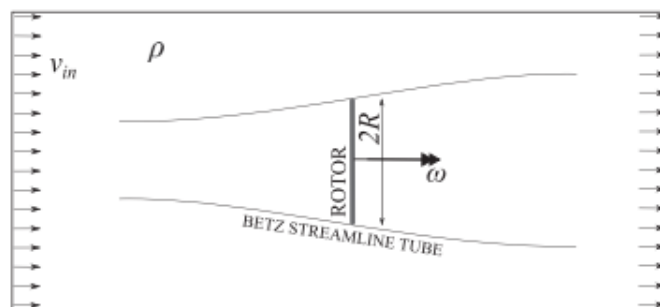


Fig. 1. Sketch of the Betz model.

The Betz model consists of an ideal circular planar turbine with radius  $R$ , traversed by an incompressible fluid flow with a rectilinear flow at constant speed, which produces a rotating turbine with an angular velocity  $\omega$ . For the theory, the power available from the fluid flow  $P_f$  is:

$$P_f = \frac{1}{2} \rho A v_{in}^3 \quad (1)$$

where  $\rho$  is the fluid density,  $A$  is the crossflow area of the turbine and  $v_{in}$  is the flow velocity of the stream. The performance coefficient is given by the ratio  $C_p = P_t/P_f$ , where  $P_t$  is the power produced by the screw turbine. Based on Betz theory, the performance coefficient has an upper limit of 0.59, but in practice some contribution of losses reduces turbine efficiency. Betz theory is widely used to evaluate the performance coefficients of wind turbines and is generally used also for more complex three-dimensional turbines. Another interesting example is provided by Schleicher *et al.* [21], who used experiments and numerical simulations to design portable micro-hydrokinetic turbines, evaluated their efficiency through Betz theory. In general, the performance coefficient is related to three main contributions: performance related to turbine characteristics  $C_{p,t}$ , losses related to transmission and support system friction  $\eta_f$ , and electrical losses to the generator or alternator  $\eta_e$ :

$$C_p = C_p \cdot t \eta_f \eta_e \quad (2)$$

The performance coefficient  $C_p$  represents the dimensionless form of the turbine power production  $P_t$ , which depends on the turbine tip speed, i.e. on the rotational speed and turbine radius. The corresponding dimensionless speed is given by the ratio  $TSR = \omega R / v_{in}$  (Speed Ratio), where  $\omega$  is the angular velocity of the rotor and  $R$  is the diameter of the rotor. As a function of TSR, the performance coefficient collapses into a curve (of course, as long as the geometry and Reynolds number range of the flow are the same). Performance coefficient curves of some turbines as a function of Speed Ratio are available in Ref. [22].

In a laboratory experiment, the Archimedes Screw turbine design can be seen in Fig. 2. The power generated is measured by a balancing system, which is connected to the turbine shaft, which slows down the rotation of the turbine. The power generated by the  $P_t$  screw turbine is obtained by multiplying the balancing force by the displacement speed due to the turbine rotation. Then the performance coefficient resulting from laboratory experiments is

$$C_{p,exp} = C_{p,t} \eta_f \quad (3)$$

where the loss of electricity is lost ( $\eta_e = 1$ ), but the friction losses due to the supporting and balancing system must be evaluated to get the efficiency of the turbine only. On the other hand, numerical simulations provide a large amount of information about the flow surrounding the turbine, including the resultant torque from the fluid pressure and the stress on the turbine surface. The product of the torque with the angular velocity giving the generated power and dividing it by the available fluid power, we get the turbine performance coefficient alone:

$$C_{p,num} = C_{p,t} \quad (4)$$

Saroinsong Tineke, *et al.* (2017) research entitled design for manufacturing Archimedes screw turbines for micro-hydro power plants. The results of this study explain that the design/model and manufacture of the Archimedes screw turbine on a laboratory scale is the Archimedes screw model made using flexglass material, the geometric shape is three blades, the screw blades are  $30^\circ$ , the number of turns is 21, the radius ratio is 0.54 with a range of  $2.4 R^0$  [24].

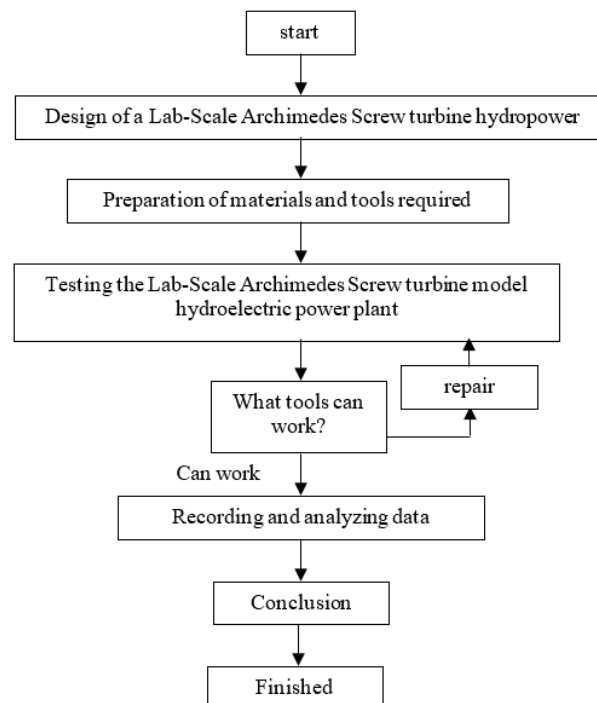


Fig. 2. Research Flowchart

Zainuri Anwar, *et al.* (2021) on the research title Archimedes screw type micro hydro turbine design with a power capacity of 560 watts. The design results show that the optimum turbine blade diameter and pitch

distance are 0.213 m and 0.312 m respectively at a turbine inlet water discharge of 0.2 m<sup>3</sup>/s and a turbine shaft output power of 563.3 Watt. Testing of the designed screw turbine was carried out in the river flow of the PuriKedaton Housing Complex, Pematang Gajah Village, Rt 13, Jambi province. The test results show that the highest turbine power occurs at a shaft loading of 30 kg with a turbine output power of 445 Watt and an efficiency of 78.9% [25].

Syahputra, T. M. (2017) with the title Design and Build of a Pico Hydro Power Plant Prototype Using a Screw Turbine. In this study, we will discuss PLTMH using an Archimedes screw turbine, where the length of the turbine used is longer than previous studies, namely 150 cm, so that the water flowing in the turbine channel can take longer to turn the turbine and can increase the efficiency of the turbine. This Archimedes screw turbine is still very rarely used in Bali. So to obtain specification data related to the Archimedes screw turbine it is difficult to obtain, therefore it is necessary to make a MHP model using this Archimedes screw turbine, so that tests can be carried out related to the parameters that affect the performance of the Archimedes screw turbine, one of which is namely the influence of water pressure [26].

From the above review, in this study we will design a laboratory-scale Archimedes Screw turbine model hydroelectric simulator with two strokes without ducts, and analyze the different performance contributions and strictly follow the theory of Archimedes Screw turbine. This study uses laboratory experiments, to determine the torque generated by the flow in the Archimedes Screw turbine.

## 2. METHODS

### 2.1. Research Stages

The drawing Fig. 3 shows how to design a laboratory-scale Archimedes Screw turbine model hydroelectric simulator system model, prepare materials and equipment, assemble a laboratory-scale Archimedes Screw turbine hydroelectric generator simulator, conduct testing of a hydroelectric model simulator. Archimedes Screw turbine laboratory scale, record and analyze. This process can be seen in the image Fig. 3.

### 2.2. Laboratory Scale Archimedes Turbine Model Simulation Design

The materials used in the design of the Archimedes Screw model hydroelectric power plant can be seen in Fig. 3 which is composed of an open channel with a small longitudinal slope, with a length of  $l = 8\text{ m}$ , a width of  $b = 0.3\text{ m}$  and a height of  $t = 0.3\text{ m}$ . The channel is made of painted zinc and the sides of the channel. The flow in the canal is generated by a pump that takes water from the drain tank and pumps it into the canal fill tank. Duct at one end to the discharge tank, while the other end is supported by two hydraulic cylinders, which allows us to vary the inclination of the duct between  $i = 0\%$  and  $i = 6.7\%$ .

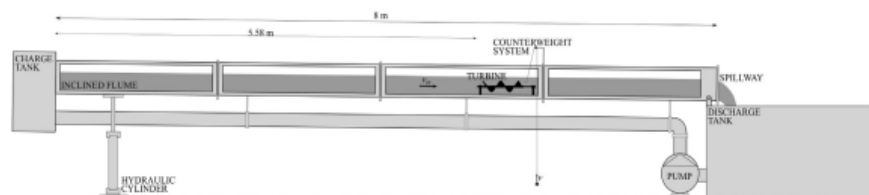


Fig. 3. Simulation Design of the Archimedes Screw Turbine Hydroelectric Power Plant

The fluid velocity  $v_{in}$  is varied by changing the flow rate in the channel and this is varied by controlling the longitudinal slope of the channel and by using different types of spillways. The slope of the channel was varied between  $i = 0.48\%$  and  $i = 2.04\%$  when using circular overflow and between  $i = 0.48\%$  and  $i = 1.6\%$  when using rectangular. The flow rate is calculated by measuring the depth of the water in the spillway and using the spillway theory. A rectangular spillway (0.15 m wide and 0.1 high from the bottom of the canal) gives a flow rate  $Q_{rect} = 8.28 \cdot 10^{-3} m^{-3} s^{-1}$ ; a circular spillway (with a diameter of 0.15 m and a height from the bottom of the canal 0.1 m) gives a flow rate  $Q_{circ} = 7.60 \cdot 10^{-3} m^{-3} s^{-1}$ . The water depth is measured for each slope, but within the range of channel slope used, the flow rate does not vary with the slope. For each configuration, the water depth  $h$  at several points along the aqueduct axis is measured and the cross-sectional average fluid velocity is evaluated as  $v_{in} = Q/lh$ . The location of the threads and the slope of the ducts were selected to have a 20 mm thick layer of water over the turbine and as far from the cargo tanks as possible, to minimize their effect on the turbine. For this reason the turbines are positioned 5.58 m downstream of the cargo tanks. The turbulence in the channel is not measured, but the Reynolds number is estimated as  $Re \leq 25000$  for all configurations, therefore the flow is assumed to be fully turbulent. The mean section flow

velocities measured at the turbine site ranged between  $v_{in} = 0.12 \text{ ms}^{-1}$  and  $v_{in} = 0.17 \text{ ms}^{-1}$  and are reported in Table 1, together with other experimental characteristics.

**Table 1.** Simulated Parallel ( $\theta = 0^\circ$ ) and Tilt ( $\theta = 10^\circ$ ) Turbine Line Speeds

No	$I$ [%]	Spillway	$Q$ [ $\text{m}^3\text{s}^{-1}$ ]	$H$ [m]	$v_{in}$ [ $\text{s}^{-1}$ ]	$P_{f,\theta=0}$ [mW]	$P_{f,\theta=10}$ [mW]
F1	0.48	Circular	$7.60 \cdot 10^{-3}$	0.206	0.1239	7.4692	12.6402
F2	0.96	Circular	$7.60 \cdot 10^{-3}$	0.195	0.1209	8.8080	14.9060
F3	1.6	Circular	$7.60 \cdot 10^{-3}$	0.179	0.1426	11.3872	19.2708
F4	2.04	Circular	$7.60 \cdot 10^{-3}$	0.17	0.1502	13.3067	22.5191
F5	0.48	Rectangular	$8.28 \cdot 10^{-3}$	0.187	0.1477	12.6532	21.4132
F6	0.96	Rectangular	$8.28 \cdot 10^{-3}$	0.177	0.156	14.9085	25.2298
F7	1.6	Rectangular	$8.28 \cdot 10^{-3}$	0.162	0.1704	19.4298	32.8813

### 2.3. Laboratory Scale Archimedes Turbine Speed Simulation

The flow strength  $p_f$  is evaluated by (1), where the area of the rotor  $A$  is approximated by the projection of the turbine volume in a plane perpendicular to the flow. In our case, the turbine rotates inside a cylindrical volume with radius  $R$  and, if the turbine axis is parallel to the flow, the cross-sectional area is a circle with radius  $R$ . If the angle of the turbine axis with the flow direction is  $\theta \neq 0$ , the cross-sectional area is  $A = R^2 \pi \cos \theta$ , where  $L$  is the length of the turbine. Therefore, varying the angle  $q$ , the flow power increases as  $A$  increases. Also for this reason, the test is run using two angles:  $\theta = 0$  (parallel configuration) and  $\theta = 10$  (tilt configuration). Larger angles have not been tested to avoid lateral flow interactions with the channel walls.

Finally, the power delivered by the Archimedes turbine is the Screw Breaker  $P_{meca} = C_{screw} n 2\pi/0$  and the hydraulic efficiency by the following equation:

$$\eta = P_{meca}/(\rho g Q H) \quad (5)$$

with  $H$  determined from the inlet and outlet water levels (see Fig. 2). More information about this experimental device can be found in [15] and in [19].

### 2.4. Laboratory Scale Archimedes Turbine Design

The design of the screw turbine used in the laboratory experiment was inspired by the Archimedean screw used in small hydroelectric power plants, which are characterized by a few meters in size. Since the turbine object of this research is structured to work without civil engineering infrastructure, we can assume that in real application the turbine dimensions depend on the size (eg water depth) of the river and can range from a few decimeters to several meters. Due to the size of the available laboratory ducts, we designed a turbine with a radius of  $0.1 \text{ m}$  and only two blade strokes. The blade is designed to withstand the action of the flow and exploit the force of the flow also in an inclined configuration. The turbine model can be seen in Fig. 3, which is made of aluminum structural shaft, which is connected with other parts: turbine tubular shaft and blades, balancing system, and supporting devices in Fig. 4(a). The turbine was composed by another tubular shaft and two-stroke blades. It is realized in two parts, which are glued together and with the structural parts using high performance glue. The hydropower screw shaft has a diameter of  $20 \text{ mm}$ , while the blade is  $5 \text{ mm}$  thick, has an outer radius of  $R = 50 \text{ mm}$  and a length of each step  $P = 160 \text{ mm}$ . The blade is not perpendicular to the axis, but is inclined by  $\alpha = 70^\circ$  to the turbine axis, facing the inflow. A summary of the main geometric parameters of the tested turbines is given in Table 2.

**Table 2.** Archimedes Screw Turbine Geometric Parameters

Parameter	Symbol	Value
Turbine radius	$R$	50 mm
Axle radius	-	20 mm
Axle length	$L$	320 mm
Blade stride	$P$	160 mm
Blade inclination with respect to axle	$\alpha$	$70^\circ$

The support device is two layer cylinders, with diameters of  $27.5 \text{ mm}$  and  $30.5 \text{ mm}$ , connected at the ends of the structural tube, which can be installed in the steel support system. The support system is made up of a steel plate  $10 \text{ mm}$  thick,  $600 \text{ mm}$  long, and  $80 \text{ mm}$  wide, holding the two tap joints by means of a small spill plate (see Fig. 4(a) and Fig. 4(b)). The underground tap connection is provided with an additional internal small pin, which prevents the turbine from sliding along its axis and getting out of the support system during

operation. The support system allows rotation of the support device (and subsequently the turbine) and locates the turbine axis at  $h_t = 89 \text{ mm}$  from the bottom of the flume. The friction between the support device and the support system cannot be neglected, but is reduced as much as possible by using a wet coating steel interface.

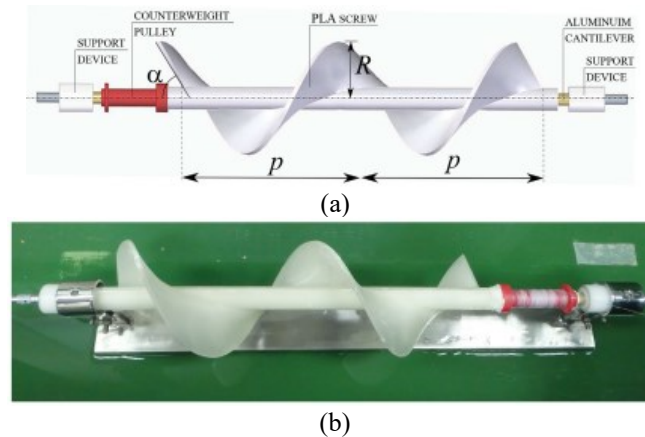


**Fig. 4.** Archimedes Screw Turbine Design Results. (a) Archimedes Screw Turbine Model Design; (b) Archimedes Screw Turbine Design Results

## 2.5. Process of Data Retrieval and Data Analysis

RSM is performed to obtain the desired response under optimal conditions in the experimental domain using the least number of experiments [27]. This method makes it possible to model and analyze problems where several factors (independent variables) affect one or more variables of interest (that is, the so-called responses) simultaneously [28]. The rope can pass over the walls of the channel via an additional pulley attached to the channel itself. The distance between the pulley and the ground (i.e. the maximum excursion of the balancing system) is  $1.5 \text{ m}$ . At the start of each test, the turbine is kept stationary and a counterweight is held a few centimeters above the ground. When the turbine is released, the video camera begins to record the displacement of the counterweight during its excursion with a frequency of  $29.97 \text{ Hz}$ . A dark panel and measuring tape are placed behind the mass to regard the mass itself as the target and measure the mass transfer in a fixed time step  $\Delta t = 250$ , during which the video is divided. Then, the lift velocity for each time step is evaluated as  $v = s/\Delta t$ . Examples related to the  $F1 - \theta 0$  test are presented in Table 3. No relevant acceleration was revealed by instrument sensitivity, although in some experiments the velocity fluctuated significantly. This indicates that the turbine rotation is not constant, but no clear trend is deduced from the entire set of experiments. Therefore, the time average over the duration of the run from the rated lift speed  $v$  is calculated. The average speed measured by this procedure corresponds to the tangential velocity of the turbine pulley and is related to the angular velocity of the turbine  $\omega$  through the relationship  $v = \omega r$ , where  $r = 7.7 \text{ mm}$  is the radius of the pulley around which the rope is wound, about the axis of the turbine. The above system allows one to evaluate the power generated when the turbine is rotated, simply by multiplying the mass's gravity by the lift speed:

$$P_t = mgv \quad (6)$$

where  $g$  is the acceleration due to gravity. Summarizing, 14 different experimental conditions are reproduced (see Table 4). Each test condition was reproduced three times to check for repeatability. The average speed over the three realizations is used to evaluate the power output  $P_t$  and, subsequently, the experimental performance coefficient  $C_{p.exp}$ . The results are summarized in Table 4, which also provides the angular velocity of the turbine  $\omega$  and TSR which will be used for comparison with other hydrokinetic turbines.

To highlight the trend in the performance coefficients, the experimental results have been divided into two groups, according to two different configurations (parallel and skewed), and the arithmetic mean of TSR and  $C_{p.exp}$  in each group has been calculated, giving  $TSR = 0.1117$  and  $C_{p.exp} = 0.12$  for flat configuration and  $TSR = 0.1112$  and  $C_{p.exp} = 0.07$  for slanted configuration.

Intact surface between the movable object (layer turbine support device) and the fixed object (steel joint). The steel-layer friction coefficient is taken to be equal to  $f = 0.04$  (as reported in some engineering handbooks) and the friction force is estimated as  $F_f = fF_s$ , where  $F_s$  is the reaction force, divided equally between the two joints:

$$F_s = \frac{(m_t - \rho V_t)g}{2} \quad (7)$$

where  $m_t = 0.325 \text{ kg}$  and  $V_t = 0.239 \cdot 10^{-3} \text{ m}^3$  are the mass and volume of the turbine, respectively, while  $\rho$  is the density of water. The reaction force is always the same for all experiments  $F_s = 0.42 \text{ N}$  and produces a friction force equal to  $F_f = 16.96 \cdot 10^{-3} \text{ N}$ . The frictional force, tangential to the surface of the joint, dissipates a force of

$$P_{diss} = F_f \omega (r_1 + r_2) \quad (8)$$

where  $r_1 = 0.01375 \text{ m}$  and  $r_2 = 0.01525 \text{ m}$  are the second radii. The power loss is reported, for each test, in the penultimate column of Table 4. The sum of the rated power  $P_{t.exp}$  and the power loss  $P_{diss}$  provides an estimate of the power output of the turbine used to evaluate the engine performance coefficient only  $C_{p,t}$  (Table 4) and extrapolating the efficiency of the support system, namely  $\eta_f = 0.574$  for all experiments. Considering the measured and dissipated power, the fixed average performance coefficient of the machine itself is  $C_{p,t} = 0.21$  for parallel configuration and  $C_{p,t} = 0.12$  for inclined configuration. The phenomenon of water overflowing is when the water flow through the screw exceeds the maximum volume of the bucket. The overflow causes a loss of power which does not assist the rotation of the turbine. Such a phenomenon is consistent with findings reported by Kathleen Songin (Songin, 2017) where water starts to overflow over the central screw shaft and flows into the downstream bucket; the water surface is disturbed by falling water (Fig. 5) [31].

### 3. RESULTS AND DISCUSSION

#### 3.1. Speed Simulation Results in the Laboratory

The results of the  $F_1 - \theta_0$  speed simulation test carried out on the Archimedes screw turbine model hydroelectric power plant, can be seen in Table 3. More accurate evaluation of the engine performance coefficient alone  $C_{p,t}$  is possible through special numerical simulations. CFD is frequently used in the literature to evaluate the performance coefficients of certain types of turbines (eg Refs [32], [33]). From the results of the speed test in Table 3, to evaluate the turbine performance coefficient alone, the geometry of the laboratory turbine is reproduced in detail, the support system and counter system are ignored and the flume is replaced with a larger fluid domain that characterizes the laboratory experiment. This larger domain, with the free slip boundary conditions, is intended to eliminate wall effects, free surfaces, and possible occlusion effects. In this way, numerical simulations provide results that cannot be strictly compared with experiments, but allow us to focus on turbine power generation only and extend turbine operating conditions to the entire possible range. In more detail, the fluid volume is  $2 \text{ m}$  long in the flow direction,  $1 \text{ m}$  wide and  $0,6 \text{ m}$  high (sketch of the horizontal domain plane for both configurations is reported in Fig. 5). The turbine is located in the center of the cross section, at a distance of  $4 R$  from the inflow boundary and  $30 R$  from the outflow boundary. For inclined turbines the same spacing is used, the center of the turbine corresponding to the center of the cross flow section.

**Table 3.** Speed Testing  $F_1 - \theta_0$

No	$t[\text{fr}]$	$v[\text{ms}^{-1}]$
1	250	$1.435 \cdot 10^{-2}$
2	500	$1.252 \cdot 10^{-2}$
3	750	$1.121 \cdot 10^{-2}$
4	1000	$1.235 \cdot 10^{-2}$
5	1250	$1.560 \cdot 10^{-2}$
6	1500	$1.605 \cdot 10^{-2}$
7	1750	$1.547 \cdot 10^{-2}$
8	2000	$1.260 \cdot 10^{-2}$
9	2250	$0.963 \cdot 10^{-2}$
10	2500	$1.131 \cdot 10^{-2}$
11	2750	$1.135 \cdot 10^{-2}$
12	3000	$1.083 \cdot 10^{-2}$
13	3250	$1.080 \cdot 10^{-2}$
14	3500	$1.221 \cdot 10^{-2}$
15	3750	$1.119 \cdot 10^{-2}$
16	4000	$1.329 \cdot 10^{-2}$
17	4250	$1.025 \cdot 10^{-2}$

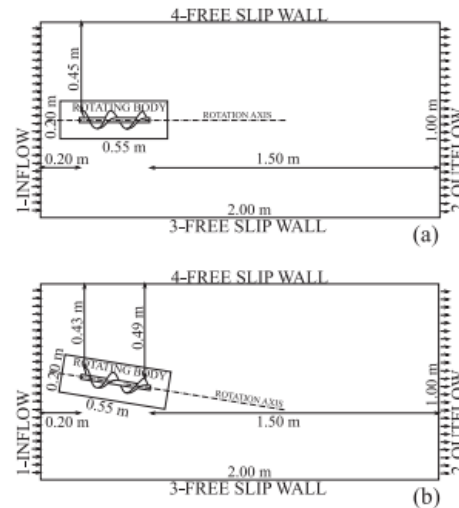


**Fig. 5.** Horizontal Plane Sketch (a) Aligned Turbine ( $\theta = 0^\circ$ ); (b) Tilt Turbine ( $\theta = 10^\circ$ ).

To produce a constant flow in the domain, the inflow and outflow boundary conditions were set at limits 1 (inflow) and 2 (outflow) of Fig. 5. To simulate conditions similar to the experiment, velocity  $v_{in} = 0.2 \text{ m s}^{-1}$  is given on the inflow and outflow limits. The free slip wall boundary conditions are defined at the other four boundaries.

The turbine is placed in the center of the cross-section, at a distance of  $4R$  from the inflow boundary and  $30R$  from the outflow boundary, to minimize the interaction of upstream and downstream hydrodynamic phenomena with the boundary [34]. For inclined turbines the same spacing is used, the center of the turbine corresponding to the center of the cross flow section.

The MRF method [35] belongs to a single domain of multiple rotating reference frames, whose interfaces are selected such that the flow field at that location is independent of the orientation of the moving parts. The computation domain is divided into sub domains, one of which rotates with respect to the other (inertial) frame. The governing equations (conservation of mass and conservation of momentum) in each subdomain are written with respect to that subdomain's frame of reference. At the boundary between two subdomains, absolute velocity continuity is enforced to provide the correct velocity value for the subdomain under consideration. The resulting flow field is a transient flow field in which the rotating parts move.

**Table 4.** Configuration and experimental results

No	$v_{in}$	$v$	$\sigma(v)$	$\omega$	$TSR$	$P_t$	$P_f$	$C_{p.exp}$	$C_{diss}$	$C_{pt}$
	$[m s^{-1}]$	$[m s^{-1}]$	$[m s^{-1}]$	$[rads^{-1}]$	$[adim]$	$[mW]$	$[mW]$	$[adim]$	$[mW]$	$[adim]$
<b>F1 – 00</b>	0.1239	$1.249 \cdot 10^{-2}$	$1.02 \cdot 10^{-3}$	1.67	0.1008	1.103	7.469	0.148	0.819	0.257
<b>F2 – 00</b>	0.1309	$1.510 \cdot 10^{-2}$	$2.18 \cdot 10^{-3}$	2.01	0.1153	1.333	8.808	0.151	0.990	0.264
<b>F3 – 00</b>	0.1426	$1.636 \cdot 10^{-2}$	$1.34 \cdot 10^{-3}$	2.18	0.1147	1.444	11.387	0.127	2.073	0.221
<b>F4 – 00</b>	0.1502	$2.052 \cdot 10^{-2}$	$4.12 \cdot 10^{-3}$	2.74	0.1366	1.812	13.307	0.136	1.345	0.237
<b>F5 – 00</b>	0.1477	$1.333 \cdot 10^{-2}$	$0.81 \cdot 10^{-3}$	1.78	0.0903	1.177	12.653	0.093	0.874	0.162
<b>F6 – 00</b>	0.156	$1.557 \cdot 10^{-2}$	$1.52 \cdot 10^{-3}$	2.08	0.0998	1.375	14.908	0.092	1.021	0.161
<b>F7 – 00</b>	0.1704	$2.114 \cdot 10^{-2}$	$1.53 \cdot 10^{-3}$	2.82	0.1241	1.867	19.430	0.096	1.386	0.167
<b>F1 – 010</b>	0.1239	$0.964 \cdot 10^{-2}$	$0.69 \cdot 10^{-3}$	1.28	0.0778	0.851	12.640	0.067	0.632	0.117
<b>F2 – 010</b>	0.1309	$1.323 \cdot 10^{-2}$	$0.93 \cdot 10^{-3}$	1.76	0.1011	1.168	14.906	0.078	0.867	0.137
<b>F3 – 010</b>	0.1426	$1.613 \cdot 10^{-2}$	$1.51 \cdot 10^{-3}$	2.15	0.1131	1.421	19.271	0.074	1.058	0.129
<b>F4 – 010</b>	0.1502	$1.948 \cdot 10^{-2}$	$1.32 \cdot 10^{-3}$	2.60	0.1297	1.720	22.519	0.076	1.277	0.133
<b>F5 – 010</b>	0.1477	$1.543 \cdot 10^{-2}$	$1.21 \cdot 10^{-3}$	2.06	0.1045	1.363	21.413	0.064	1.012	0.111
<b>F6 – 010</b>	0.156	$1.937 \cdot 10^{-2}$	$1.42 \cdot 10^{-3}$	2.58	0.1242	1.710	25.230	0.068	1.270	0.118
<b>F7 – 010</b>	0.1704	$2.271 \cdot 10^{-2}$	$2.58 \cdot 10^{-3}$	3.03	0.1333	2.005	32.881	0.061	1.489	0.106

For the problem under discussion, the rotary portion of the domain, hereinafter referred to as the rotary body, is a cylindrical volume with a radius twice the turbine diameter and a length of  $0.55 \text{ m}$ , which contains the turbine and has a common turbine axis. This configuration was chosen to reduce the rotating effect on the turbine limit hydrodynamics (and subsequently on the generated torque) and to optimize. The remainder is complementary to the fluid domain. The results separately of the two sections and rotation of the turbine are simulated driving a rotating body at each time step with a set angular velocity  $\omega$ . The solutions of the two

domains are calculated in different reference frames for each section and the boundary conditions for the inner rotating body are evaluated by interpolation of the outer body.

### 3.2. Discussion of Laboratory Experiment Simulator

Every ten time steps, i.e. every 0.2 seconds, the torque produced by the fluid in the turbine  $M_t$  is evaluated as the torque due to pressure and shear stress acting on the entire surface of the turbine with respect to the turbine axis. Fig. 6(a) and Fig. 6(b) illustrate the torque evolution in time for all simulations.

The numerical model is a pressure-based model that solves the discretized form of the Navier Stokes Mean Reynolds Equation. The turbulence model used to close the equation is Menter's  $k - \omega$  Shear Stress Transport ( $k - \omega SST$ ) model, which performs well with adverse pressure gradients and separate flows (see Refs [36]-[38] for details). This numerical model is commonly used and validated in the study of duct turbines and pumps as turbines. See for example [37]-[41].

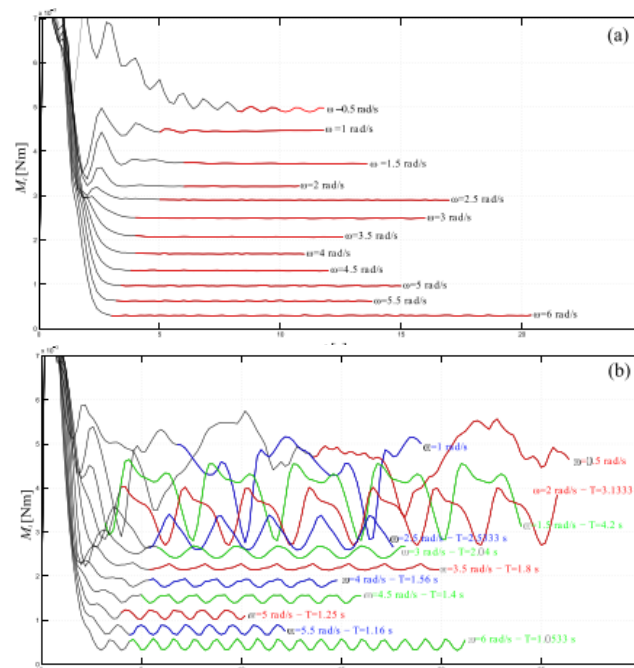


**Fig. 6.** Graph of Torque Generated by Fluid in Turbine  $M_t$ : (a) parallel turbine ( $\theta = 0^\circ$ ); (b) inclined turbine ( $\theta = 10^\circ$ ).

It is described that during the initial stages the peak shifts, which are caused by transients during the hydrodynamics of the fluid-structure interaction progress from zero to a stable state. The time required to reach the apparent state (periodic oscillations in the oblique configuration) varies between 3 seconds and 5 seconds. Results at this stage were ignored in subsequent analyses. Furthermore, for the inclined turbine, the torque evolution featuring periodic oscillations for  $\omega \geq 1.5 \text{ rad/s}^{-1}$  and the torque oscillation period  $T$  are evaluated and reported in Figure 7b for each simulation. This period corresponds to the relation  $1/T = \omega/2\pi$ , which is the turbine rotation period.

The periodic stage has been highlighted in color in Fig. 6 and these stages are used to evaluate the average torque time  $M_t$ . The achievement of a steady state is defined in two different ways, depending on the shape of the signal. In the case of a time invariant signal, such as Fig. 6(a), we require that the actual value of the variable will be within the tolerance of  $10^{-4} \text{ Nm}$  of the time invariant value. For a periodic function, as in Fig. 6(b), we apply a Matlab routine to characterize the periodicity property (period and amplitude) and, starting from the end of the time series, move backwards in time until the property remains within the tolerance of  $10^{-4} \text{ Nm}$ .

The generated power  $P_t$  can be seen in Fig. 7, which shows that they are similar for the two configurations. The best fit of each configuration is obtained using Nonlinear Least Squares (NLS) regression, which solves the problem of fitting data nonlinearly in the least squares sense with a cubic function passing through the origin. The evaluated  $f_t$  function is:  $P_t = 3.22 \cdot 10^{-2} \omega^3 - \omega^2 + 5.2 \omega \text{ mW}$  for average configuration and  $P_t = 2.66 \cdot 10^{-2} \omega^3 - 0.95 \omega^2 + 5.2 \omega \text{ mW}$  for the oblique configuration, where  $\omega$  is at  $\text{rad/s}^{-1}$ .

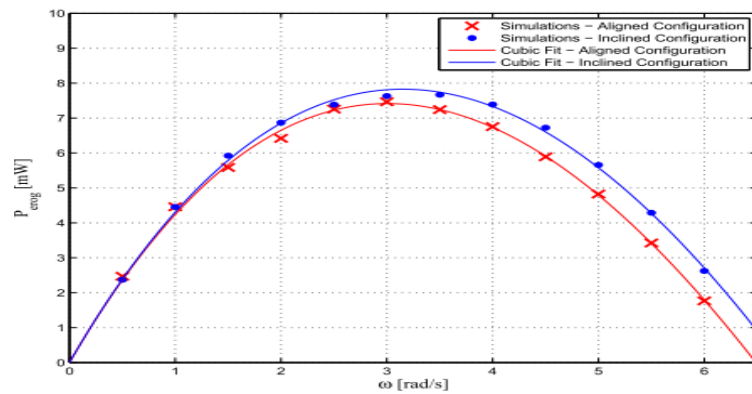


Fig. 7. Power Generated From the Corresponding Angular Velocity  $\omega$ .

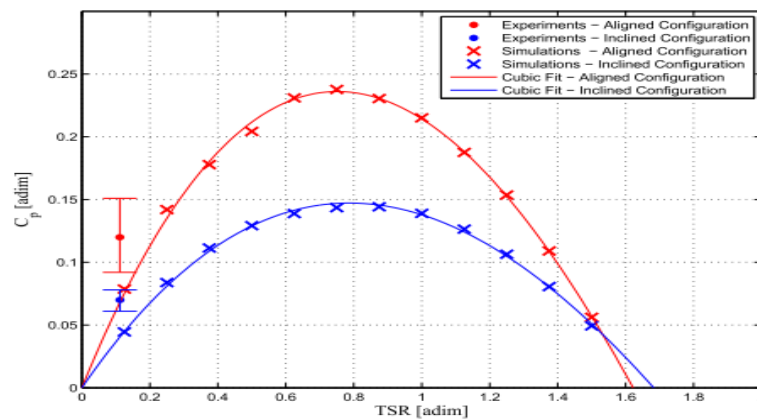


Fig. 8. Results of  $C_p$  Power Coefficient Laboratory Experiments

The performance coefficient, then, is evaluated as  $C_{p,num} = P_t/P_f$ , where the flow strength  $P_f$  is evaluated by (1) using the inflow-outflow velocity simulation, and it is equal to  $P_{f,\theta=0} = 31.42 \text{ mW}$  for flat configuration and  $P_{f,\theta=10} = 53.17 \text{ mW}$  for inclined configuration. The performance coefficients of the two configurations are shown in Fig. 8. Also for the performance coefficients, the best fit is obtained for each configuration, using Nonlinear Least Squares (NLS) regression. The  $f_t$  function that is evaluated is:  $C_p = 0.0656TSR^3 - 0.5166TSR^2 + 0.6653TSR$  for an even configuration and  $C_p = 0,0321TSR^3 - 0,2881TSR^2 + 03939TSR$  for an inclined configuration. For comparison, also our laboratory results are reported in Fig. 8.

#### 4. CONCLUSION

From the results of the research conducted there are several conclusions. The performance coefficient of the ductless screw turbine was evaluated, strictly speaking, for a fixed geometry and found to be comparable to other hydrokinetic turbines characterized by the same speed. The tilted configuration gives slightly worse performance than the paralleled configuration, due to its small performance coefficient and for the torque period it produces, it still requires detailed analysis; The proposed geometry can be used in real-life applications, providing 0.5 kW at flow velocities between 1 and 2 m/s.

For this reason, Archimedes turbines in real-life applications are a good reference for the development of simple and inexpensive devices, which minimize environmental impact and are reliable in variable water depths. Analysis is ongoing to further investigate the performance of this turbine in a tilt configuration.

#### Acknowledgments

Thank you to the editors and reviewers for all the suggestions, input and assistance in the process of publishing the manuscript. Acknowledgments are also addressed to those who have supported the research and provided moral and material assistance.

## REFERENCES

- [1] United Nations, "Resolutions and Decisions Adopted by the General Assembly during its Seventieth Session," vol. 1, 2016. <https://doi.org/10.18356/25329765-en>.
- [2] A. Nugraha, D. S. H. Silalahi, P. R. Ansyah, M. N. Ramadhan, A. Amrullah, and G. R. Cahyono, "An experimental study of the effect of variation of impact levels on working efficiency of archimedes screw turbine on micro-hydro power plant," *International Journal of Mechanical Engineering Technologies and Applications*, vol. 4, no. 1, pp. 1-9, 2023, <https://doi.org/10.21776/MECHTA.2023.004.01.1>.
- [3] H. J. Vermaak, K. Kusakana, S. P. Koko, "Status of micro-hydrokinetic river technology in rural applications: a review of literature," *Renew. Sustain. Energy Rev.* vol. 29, pp. 625-633, 2014, <https://doi.org/10.1016/j.rser.2013.08.066>.
- [4] K. Kusakana, H. J. Vermaak, "Feasibility study of hydrokinetic power for energy access in rural South Africa," in *Proceedings of the IASTED Asian Conference, Power and Energy System*, pp. 433-438, 2012, <https://doi.org/10.2316/P.2012.768-071>.
- [5] K. Kusakana, H. J. Vermaak, "Hydrokinetic power generation for rural electricity supply: case of South Africa," *Renew. Energy*, vol. 55, pp. 467-473, 2013, <https://doi.org/10.1016/j.renene.2012.12.051>.
- [6] T. Price, D. Probert, "Harnessing hydropower: a practical guide," *Appl. Energy*, vol. 57, no. 2-3, pp. 175-251, 1997, [https://doi.org/10.1016/S0306-2619\(97\)00033-0](https://doi.org/10.1016/S0306-2619(97)00033-0).
- [7] I. G. W. Putra, A. I. Weking, L. Jasa, "Analysis of the Effect of Water Pressure on the Performance of PLTMH Using Archimedes Screw Turbine," *Electrical Technology Scientific Magazine*, vol. 17, no. 3, 2018, <https://doi.org/10.24843/MITE.2018.v17i03.P13>.
- [8] M. J. Khan, M. T. Iqbal, J. E. Quaicoe, "River current energy conversion systems: progress, prospects and challenges," *Renew. Sustain. Energy Rev.*, vol. 12, no. 8, pp. 2177-2193, 2008, <https://doi.org/10.1016/j.rser.2007.04.016>.
- [9] M. J. Khan, G. Bhuyan, M. T. Iqbal, J. E. Quaicoe, "Hydrokinetic energy conversion systems and assessment of horizontal and vertical axis turbines for river and tidal applications: a technology status review," *Appl. Energy*, vol. 86, no. 10, pp. 1823-1835, 2009, <https://doi.org/10.1016/j.apenergy.2009.02.017>.
- [10] D. Kumar, S. Sarkar, "A review on the technology, performance, design optimization, reliability, techno-economics and environmental impacts of hydrokinetic energy conversion systems," *Renew. Sustain. Energy Rev.*, vol. 58, pp. 796-813, 2016, <https://doi.org/10.1016/j.rser.2015.12.247>.
- [11] A. C. Fernandes, A. B. Rostami, "Hydrokinetic energy harvesting by an innovative vertical axis current turbine," *Renew. Energy*, vol. 81, pp. 694-706, 2015, <https://doi.org/10.1016/j.renene.2015.03.084>.
- [12] A. B. Rostami, M. Armandei, "Renewable energy harvesting by vortex-induced motions: review and benchmarking of technologies," *Renew. Sustain. Energy Rev.*, vol. 70, pp. 193-214, 2017, <https://doi.org/10.1016/j.rser.2016.11.202>.
- [13] Archimede screw hydro turbine. (Accessed 24 October 2018). <https://www.renewablesfirst.co.uk/home/renewable-energy-technologies/hydropower/hydropower-learning-centre/archimede-screw-hydro-turbine/>.
- [14] D. K. Okot, "Review of small hydropower technology," *Renew. Sustain. Energy Rev.*, vol. 26, pp. 515-520, 2013, <https://doi.org/10.1016/j.rser.2013.05.006>.
- [15] W. Schleicher, H. Ma, J. Riglin, Z. Kraybill, W. Wei, R. Klein, A. Oztekin, "Characteristics of a micro-hydro turbine," *J. Renew. Sustain. Energy*, vol. 6, p. 013119, 2014, <https://doi.org/10.1063/1.4862986>.
- [16] A. Stergiopoulou, V. Stergiopoulos, E. Kalkani, "Computational fluid dynamics study on a 3d graphic solid model of archimede screw turbines," *Fresenius Environ. Bull.*, vol. 23, no. 11, pp. 2700-2706, Nov. 2014, [https://www.prt-parlar.de/download\\_feb\\_2014/](https://www.prt-parlar.de/download_feb_2014/).
- [17] A. Stergiopoulou, V. Stergiopoulos, E. Kalkani, "Experimental and theoretical research of zero head innovative horizontal axis archimede screw turbines," *Int. J. Energy Environ.*, vol. 6, no. 5, pp. 471-478, 2015, [https://www.ijee.ieefoundation.org/vol6/issue5/IJEE\\_05\\_v6n5.pdf](https://www.ijee.ieefoundation.org/vol6/issue5/IJEE_05_v6n5.pdf).
- [18] Z. Anwar, B. S. Parsarwan, E. Sunarso, "Design of Archimedes Screw Microhydro Turbine with 560 Watt Power Capacity," *Journal of Electrical Power Control and Automation*, vol. 4, no. 1, pp. 29-34, 2021, <https://doi.org/10.33087/jepca.v4i1.43>.
- [19] A. Betz, "Das maximum der theoretischmöglichenausnützung des windesdurchwindmotoren," *Zeitschrift für das gesamte Turbinenwesen*, vol. 26, pp. 307-309, 1920, <https://cir.nii.ac.jp/crid/1570572701389062144>.
- [20] A. Betz, "The maximum of the theoretically possible exploitation of wind by means of a wind motor," *Wind Eng.*, vol. 37, no. 4, pp. 441-446, 2013, <https://doi.org/10.1260/0309-524X.37.4.441>.
- [21] W. C. Schleicher, J. D. Riglin, A. Oztekin, "Numerical characterization of a preliminary portable microhydrokinetic turbine rotor design," *Renew. Energy*, vol. 76, pp. 234-241, 2015, <https://doi.org/10.1016/j.renene.2014.11.032>.
- [22] M. Ragheb, A. Ragheb, "Wind turbines theory the betz equation and optimal rotor tip speed ratio," in *Fundamental and Advanced Topics in Wind Power*, vol. 1, no. 1, pp. 19-38, 2011, <https://doi.org/10.5772/21398>.
- [23] M. H. Basri, M. Bahrullah, A. Herlin, "Design of 3 Phase Generator in Gravitation Water Vortex Power Plant (GWVPP)," *Journal of Mechanical Engineering Elements.*, vol. 7, no. 1, pp. 46-53, 2020, [https://irisbang.unuja.ac.id/media/arsip/berkas\\_penelitian/38\\_Q3A230y.pdf](https://irisbang.unuja.ac.id/media/arsip/berkas_penelitian/38_Q3A230y.pdf).
- [24] T. Saroinsong, A. Thomas, and A. N. Mekel, "Design and Manufacture of Archimedes Thread for Micro-hydro Power Plants," *Prosiding Sentrinov*, vol. 3, no. 3, pp. 159-169, 2017, <http://proceeding.sentrinov.org/index.php/sentrinov/article/view/283>

- [25] Z. Anwar, B. S. Parsaroan, E. Sunarso, "Design of Archimedes Screw Micro Hydro Turbine with 560 Watt Power Capacity," *Journal of Electrical Power Control and Automation*, vol. 4, no. 1, pp. 29-34, 2021, <https://doi.org/10.33087/jepca.v4i1.43>.
- [26] T. M. Syahputra, "Design of a Pico Hydro Power Plant Prototype Using a Screw Turbine," *KITEKTRO: Jurnal Online Teknik Elektro*, vol. 2, no. 1, pp. 16-22, 2017, [http://etd.unsyiah.ac.id/index.php?p=show\\_detail&id=30936](http://etd.unsyiah.ac.id/index.php?p=show_detail&id=30936).
- [27] M. A. Bezerra, S. L. C. Ferreira, C. G. Novaes, A. M. P. Dos Santos, G. S. Valasques, U. M. F. da Mata Cerqueira, J. P. dos Santos Alves, "Simultaneous optimization of multiple responses and its application in analytical chemistry: a review," *Talanta*, vol. 194, pp. 941-959, 2019, <https://doi.org/10.1016/j.talanta.2018.10.088>.
- [28] D. C. Montgomery. *Introduction to Statistical Quality Control*. John Wiley & Sons, 2019, <https://books.google.co.id/books?id=oh7zDwAAQBAJ&dq=Introduction+to+Statistical+Quality+Control>.
- [29] G. Dellinger, A. Terfous, P.A. Garambois, A. Ghenaim, "Experimental investigation and performance analysis of archimedes screw generator," *Journal of Hydraulic Research*, vol. 54, no. 2, pp. 197-209, 2015, <https://doi.org/10.1080/00221686.2015.1136706>.
- [30] G. Dellinger. "Etude experimentale et optimisation des performances hydrauliques des vis d'archimedeutilises dans les micro centraleshydroelectriques," *Doctoral dissertation, Université de Strasbourg*, 2015, <https://hal.science/tel-01355570/>.
- [31] K. Songin, "Experimental Analysis of Archimedes Screw Turbines," *Doctoral dissertation, University of Guelph*, 2017, <https://atrium.lib.uoguelph.ca/items/8989877c-530c-4b3b-94fb-9d807818da6f>.
- [32] W. Schleicher, H. Ma, J. Riglin, Z. Kraybill, W. Wei, R. Klein, A. Oztekin, "Characteristics of a micro-hydro turbine," *J. Renew. Sustain. Energy*, vol. 6, p. 013119, 2014, <https://doi.org/10.1063/1.4862986>.
- [33] A. Kumar, R. P. Saini, "Performance analysis of a savonius hydrokinetic turbine having twisted blades," *Renew. Energy*, vol. 108, pp. 502-522, 2017, <https://doi.org/10.1016/j.renene.2017.03.006>.
- [34] L. P. Chamorro, C. Hill, S. Morton, C. Ellis, R. E. A. Arndt, F. Sotiropoulos, "On the interaction between a turbulent open channel flow and an axial-flow turbine," *J. Fluid Mech.*, vol. 716, pp. 658-670, 2013, <https://doi.org/10.1017/jfm.2012.571>.
- [35] *ANSYS Fluent Tutorial Guide 18.0*, ANSYS, Inc. Release, 2017, <http://users.abo.fi/rzevenho/ansys%20fluent%2018%20tutorial%20guide.pdf>.
- [36] B. Andersson, R. Andersson, L. Håkansson, M. Mortensen, R. Sudiyo, B. Van Wachem. *Computational Fluid Dynamics for Engineers*. Cambridge University Press, 2011, [https://books.google.co.id/books?hl=id&lr=&id=A\\_g5016wS-0C](https://books.google.co.id/books?hl=id&lr=&id=A_g5016wS-0C).
- [37] F. R. Menter, "Improved Two-Equation K-Omega Turbulence Models for Aerodynamic Flows," *NASA Technical*, No. A-92183, 1992, <https://ntrs.nasa.gov/citations/19930013620>.
- [38] F. R. Menter, "Two-equation eddy-viscosity turbulence models for engineering applications," *AIAA J.*, vol. 32, no. 8, pp. 1598-1605, 1994, <https://doi.org/10.2514/3.12149>.
- [39] T. Lei, Y. Zhiyi, X. Yun, L. Yabin, C. Shuliang, "Role of blade rotational angle on energy performance and pressure fluctuation of a mixed-flow pump," *Proc. IME J. Power Energy*, vol. 231, no. 3, pp. 227-238, 2017, <https://doi.org/10.1177/0957650917689948>.
- [40] Y. Hao, L. Tan, "Symmetrical and unsymmetrical tip clearances on cavitation performance and radial force of a mixed flow pump as turbine at pump mode," *Renew. Energy*, vol. 127, pp. 368-376, 2018, <https://doi.org/10.1016/j.renene.2018.04.072>.
- [41] Y. Liu, L. Tan, "Tip clearance on pressure fluctuation intensity and vortex characteristic of a mixed flow pump as turbine at pump mode," *Renew. Energy*, vol. 129, pp. 606-615, 2018, <https://doi.org/10.1016/j.renene.2018.06.032>.
- [42] T. Lei, X. Zhifeng, L. Yabin, H. Yue, X. Yun, "Influence of t-shape tip clearance on performance of a mixed-flow pump," *Proc. IME J. Power Energy*, vol. 232, no. 4, pp. 386-396, 2018, <https://doi.org/10.1177/0957650917733129>.
- [43] M. Liu, L. Tan, S. Cao, "Theoretical model of energy performance prediction and bep determination for centrifugal pump as turbine," *Energy*, vol. 172, pp. 712-732, 2019, <https://doi.org/10.1016/j.energy.2019.01.162>.

## BIOGRAPHY OF AUTHORS



**Muhammad Hasan Basri**, Received a Bachelor's degree in Mechanical Engineering from the Malang National Institute of Technology (2008), a Masters in FMIPA Science from the SepuluhNopember Institute of Technology, Surabaya (2015). Since 2018 joined the Faculty of Engineering, Nurul JadidPaiton University Indonesia as a Lecturer. As a member of Fortei 7, and his area of interest is in renewable energy and its applications.



**Ahmad Muhtadi**, He holds a Bachelor's degree in Electrical Engineering from the Nurul Jadid College of Technology (2017), and a Masters in Electrical Engineering from the University of Jember (2022). Since 2018 he has joined the Faculty of Engineering, University of Nurul Jadid Paiton Indonesia as an Assistant Lecturer.



**Darul Hasan**, Born in Probolinggo, on November 11, 1999. The author is a student of the Electrical Engineering Study Program, Faculty of Engineering, Nurul Jadid University. The author has the field of Renewable Energy.